Navigation by Path Integration and the Fourier Transform: A Spiking-Neuron Model

Jeff Orchard[1,2], Hao Yang[2], and Xiang Ji[1,2]

[1] Cheriton School of Computer Science
[2] University of Waterloo
jorchard@uwaterloo.ca

Abstract. In 2005, Hafting et al [1] reported that some neurons in the entorhinal cortex (EC) fire bursts when the animal occupies locations organized in a hexagonal grid pattern in their spatial environment. Previous to that, place cells had been observed, firing bursts only when the animal occupied a particular region of the environment. Both of these types of cells exhibit theta-cycle modulation, firing bursts in the 4-12Hz range. In addition, grid cells fire bursts of action potentials that precess with respect to the theta cycle, a phenomenon dubbed "theta precession". Since then, various models have been proposed to explain the relationship between grid cells, place cells, and theta precession. However, most models have lacked a fundamental, overarching framework. As a reformulation of the pioneering work of Welday et al [2], we propose that the EC is implementing its spatial coding using the Fourier Transform. We show how the Fourier Shift Theorem relates to the phases of velocity-controlled oscillators (VCOs), and propose a model for how various other spatial maps might be implemented. Our model exhibits the standard EC behaviours: grid cells, place cells, and phase precession, as borne out by theoretical computations and spiking-neuron simulations. We hope that framing this constellation of phenomena in Fourier Theory will accelerate our understanding of how the EC – and perhaps the hippocampus – encodes spatial information.

1 Introduction

Some neurons in the entorhinal cortex (EC), called "grid cells", spike preferentially when the animal is at points arranged in a hexagonal grid pattern [1]. Figure 1 shows the output of a sample place cell, taken from [3]. Neurons in the hippocampus, called "place cells", were found to activate when the animal was in a particular location in the environment (see Fig. 1). Both types of cells, place cells and grid cells, are modulated by the theta rhythm, a pattern of activity that oscillates at between 4 and 12 Hz.

Researchers proposed that the grid patterns might arise from an interference pattern between neural oscillators. This is made possible by *velocity-controlled oscillators*, or *VCO*s. A VCO is a neuron or population of neurons whose activity

O. Zaïane and S. Zilles (Eds.): Canadian AI 2013, LNAI 7884, pp. 138–149, 2013.

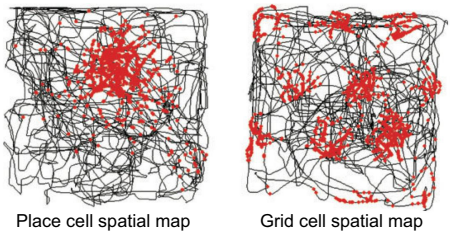

Fig. 1. Action potentials (red dots) superimposed on a rat's path, showing the output of a place cell (left) and a grid cell (right). From [3].

oscillates, but at a frequency that is modulated by velocity. As the animal moves, these VCOs take on slightly different frequencies. If the frequency of the VCOs are *linear* functions of velocity, then as the animal moves the phase difference between two VCOs can be written

$$\phi(t) = \int_0^t c_1 v(\tau) - c_2 v(\tau) d\tau = (c_1 - c_2) \int_0^t v(\tau) d\tau = (c_1 - c_2)\, x(t) \ ,$$

where c_1 and c_2 are scalar constants. Hence the phase difference $\phi(t)$ is proportional to total displacement $x(t)$. In this way, the phase differences between VCOs encodes the rat's position. This is an important point that we will come back to later.

We can think of the state of a VCO as a rotating unit vector, called its *phase vector*. By combining (adding) the phase vectors from two VCOs with different frequencies, the result is a beat interference pattern that generates periods of constructive and destructive interference as their phase difference evolves [4]. Since phase and position are tied together, this interference pattern overlays the animal's spatial environment. Combining three VCOs (that differ in preferred direction by multiples of 120°) tends to create a hexagonal grid interference pattern [5,6].

How are place cells and grid cells related? As recently as 2008, researchers had only a handful of ideas of how grid cells might combine to produce place cells [3]. But a consensus seems to be that place-cell like behaviour results from adding together a number of grid cells [7,8,9,10,11]. A comprehensive review of the various proposed models can be found in [12].

A rather different model, not based on oscillators, used Gaussian surfaces to represent place cells, but encoded these Gaussians by their Fourier coefficients [13]. Their spiking-neuron implementation uses an approximation of the Fourier Shift Theorem (discussed later), moving the Gaussian pattern of excitation around by applying phase shifts to the Fourier coefficients. However, their model does not address grid cells.

In 2011, Welday et al [2] proposed a more complete theory of the mechanisms combining grid cells, place cells, and phase precession. Their model involves a bank of VCOs arranged in a 2-dimensional (2-D) array as shown in the left pane of Fig. 2. In their firing-rate model, each VCO is as a ring oscillator with a wave of

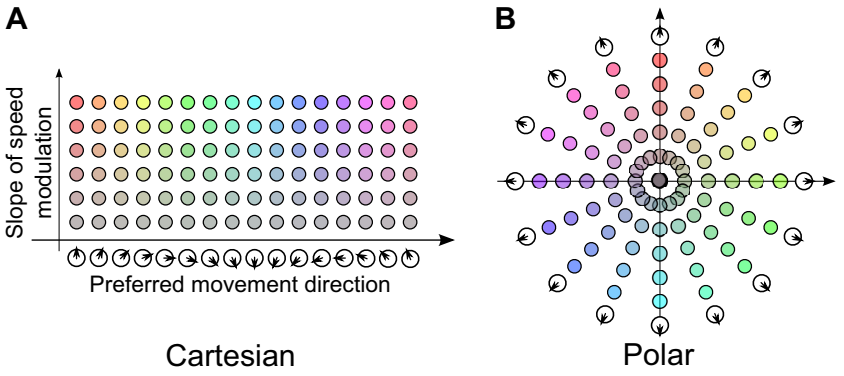

Fig. 2. Cartesian versus polar representation of VCOs. The Cartesian arrangement is derived from part of Fig. 7 in [2]. The polar arrangement consists of a number of "propellers", lines of VCOs that pass through the origin.

activity that cycles at (or near) theta frequency. Hence, each neuron on the ring activates at a particular phase. According to their paper, connecting a read-out node to all the oscillators of a given row produces a place cell. Similarly, choosing only three oscillators from a row, but with preferred directions separated by 120°, yields a grid cell. Finally, choosing all the oscillators with the same preferred direction vector can generate a border cell.

While the ideas presented in that paper have merit, the authors' explanations for their claims are somewhat disconnected and hard to follow. In this paper, we bring together those multiple fragments of theory and re-formulate them into a coherent and elegant framework using Fourier Theory. We also extend the model and hypothesize a separation of labour, where location is encoded using VCO phase, and spatial map patterns are encoded using connection weights.

2 Fourier Model

The bank-of-oscillators model states that a VCO's frequency depends on two parameters: the speed of the animal, and the cosine of the animal's velocity vector with the VCO's preferred direction. Plotting those two factors on axes arranges the VCOs into a 2-D Cartesian space, as shown in Fig. 2A.

Another, perhaps more intuitive way of presenting the same 2-D parameter space is to use polar coordinates, as shown in Fig. 2B. In this view, the direction of displacement from the origin indicates the preferred direction, and the distance from the origin gives the gain of the frequency modulation. Consider a VCO located a position $\mathbf{c}$ in the plane. In this arrangement, the animal moving at velocity $\mathbf{v}$ makes the VCO located at position $\mathbf{c}$ oscillate with frequency $\mathbf{c} \cdot \mathbf{v} + \theta$, where θ is the baseline frequency. This is consistent with the cosine frequency tuning with respect to preferred direction [2].

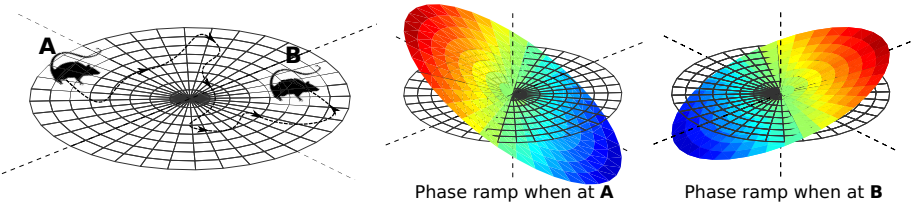

Fig. 3. As the rat moves from position A to position B, the phase ramp changes its slope

Consider the phase difference between the VCO at the origin, and one located at $\mathbf{c}$,

$$\phi(t) = \int_0^t (\mathbf{c} \cdot \mathbf{v}(\tau) + \theta) - \theta d\tau \;=\; \mathbf{c} \cdot \int_0^t \mathbf{v}(\tau) d\tau \;=\; \mathbf{c} \cdot \mathbf{x}(t) \;,$$

where $\mathbf{v}(t)$ is the animal's velocity at time t. This is a dot-product, and is linear in $\mathbf{c}$. To see this, fix a location $\mathbf{x}$ and plot the phase difference for all locations $\mathbf{c}$; this forms a plane as shown in Fig. 3. Moreover, the slope of the ramp encodes $\mathbf{x}$, the location of the animal. As the animal moves from one place to another, the phase ramp tilts to track its location.

These VCOs connect to read-out nodes, including place cells, grid cells, etc. We will refer to these read-out nodes as *spatial-map* nodes, since they draw a map of activity as the animal wanders through its space.

To understand how this ramp can be used to generate spatial maps, we need to know a bit about the Fourier transform. In the following sections, we review the Fourier transform and outline the benefits of thinking about the EC in terms of the this powerful mathematical tool.

2.1 Fourier Theory Basics

We will develop our argument using the Discrete Fourier Transform (DFT). Consider a sampled function f_n with N samples indexed $n = 0, \ldots, N-1$. The DFT of f is

$$F_k = \sum_{n=0}^{N-1} f_n \exp\left(-2\pi i \frac{nk}{N}\right) \;,\; k = 0, \ldots, N-1 \,. \tag{1}$$

Each complex number F_k is called a Fourier coefficient. We can also denote the transform using $F = \mathrm{DFT}(f)$. In essence, the DFT is a frequency decomposition; it takes a spatial signal and represents it as a sum of wave fronts of various frequencies (and orientations, in 2-D and higher). Each Fourier coefficient occupies a different location in the frequency domain, and each location represents a different wave front. The value of a Fourier coefficient, F_k, represents the contribution of its wave front. The coefficient F_0 has a special name; it is called the DC, and it is located at the origin of the frequency domain.

The Fourier basis functions in (1) are N-periodic. If we also assume that f is periodic (i.e. $f_{-1} = f_{N-1}$, as is convention), then the DFT can equivalently be written,

$$F_k = \sum_{n=-\tilde{N}}^{\tilde{N}} f_n \exp\left(-2\pi i \frac{nk}{N}\right) \ , \ k = -\tilde{N}, \ldots, \tilde{N} \ ,$$

where we assume for simplicity – but without loss of generality – that N is odd, and use the symbol $\tilde{N}$ to represent $\lfloor \frac{N}{2} \rfloor$, where the delimiters $\lfloor \cdot \rfloor$ denote rounding toward zero. We will use this equivalent, centred version of the DFT throughout this paper.

The Fourier Shift Theorem tells us how shifting (translating) a signal influences its Fourier coefficients. Suppose that F_k are the Fourier coefficients of a signal f_n. Consider a shifted version, f_{n-d}, and its Fourier coefficients, G_k. The relationship between G_k and F_k is

$$G_k = \exp\left(-2\pi i \frac{dk}{N}\right) F_k \qquad , \ k = -\tilde{N}, \ldots, \tilde{N} \ .$$

Thus, the Fourier coefficients of the shifted signal can be derived from the coefficients of the original signal multiplied by a phase-shift, where the amount of the phase-shift is a linear function of the frequency index k. The Fourier Shift Theorem even works for non-integer values of d, and in higher dimensions where dk turns into a dot-product between a shift vector, d, and a coordinate in the frequency domain, k.

2.2 Entorhinal Cortex

We propose that the polar arrangement in Fig. 2B is a 2-D frequency domain, and each VCO corresponds to a Fourier coefficient. This formulation splits the production of spatial maps into two components: the spatial pattern of the map, versus movement throughout that map.

Movement throughout the map is taken care of by the phases of the VCOs. As the rat moves around, the VCOs form a phase ramp. This phase ramp is used to shift the spatial map, just like the Fourier Shift Theorem does.

The spatial map itself comes from connection weights. Consider the set of neural connections between a VCO and a spatial-map (read-out) node. Those connections transform the VCO's phase vector and contribute the result to the map node. Since the VCOs generate Fourier basis functions (sines and cosines), this projection to the spatial-map node is tantamount to performing an inverse Fourier transform. Figure 4 illustrates different spatial maps resulting from different selections of VCOs. In that figure, one can think of the inclusion/exclusion of the VCOs as connection weights of all 1s, or all zeros, respectively. Other spatial maps can be realized by choosing different connection weights, as illustrated in Fig. 4D. Though not shown here, border cells (as discussed in [2]) can also be implemented using the same techniques.

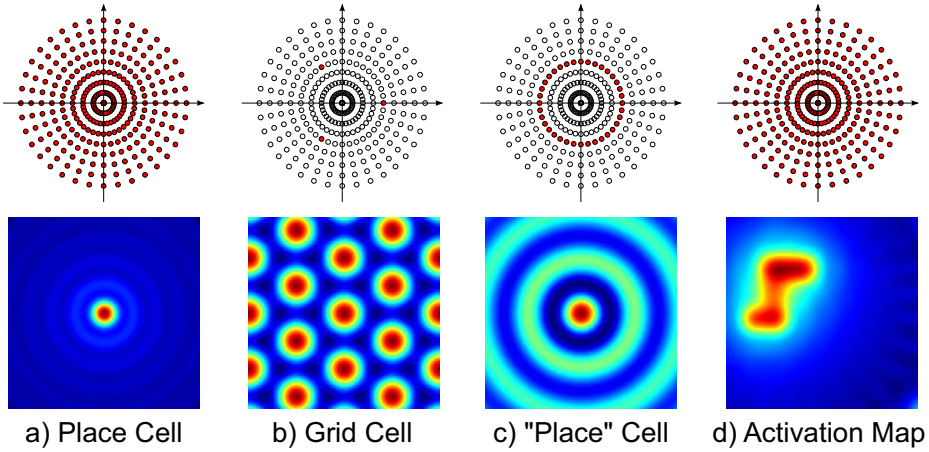

Fig. 4. Sample spatial maps (bottom row) and the VCOs used to generate them (top row). For comparison, we included C to show the "place" cell that was proposed in [2]. D shows a general spatial activation map, created by using the Fourier coefficients of an ideal spatial map to set connection weights from a bank of VCOs (18 propellors, 9 rings) to a readout node.

This Fourier interpretation splits the generation of spatial maps into two parts: the VCO phases form a phase ramp, and the neural connections can be interpreted as Fourier coefficients. Together, they constitute an inverse Fourier transform that generates a shifted spatial map, shifted according to the slope of the phase ramp. The beauty is that all spatial maps are shifted at the same time, all driven by the same bank of VCOs.

3 Material and Methods

We implemented a version of the EC Fourier model using spiking leaky integrate-and-fire (LIF) neurons [14]. Here we describe our implementation of the model, outline the challenges, and display results from simulation experiments.

3.1 Oscillators

To build our neural network, we used the Neural Engineering Framework (NEF) [15], a powerful and versatile platform that has proven useful for large-scale cognitive modelling [16]. Explanation of the NEF is beyond the scope of this paper, but we include a brief description.

In the NEF, information is represented in the firing rates of populations of spiking LIF neurons. That data can be extracted and transformed using optimal linear decoders. Moreover, recurrent networks can be designed to implement particular dynamical systems. For example, we used populations of 300 LIF neurons to implement the VCOs as simple harmonic oscillators, storing (x, y, θ)

in each population. Recurrent connection weights were chosen so that the (x, y) state oscillates with frequency θ. We used a normalized version of the simple harmonic oscillator by forcing (x, y) to be a unit-vector.

We constructed arrays of 17 VCOs to form propellers, like those seen in the polar arrangement in Fig. 2B. As the arrangement dictates, the degree to which the animal's velocity vector influences the VCOs frequency depends on its location in the plane. Given a 2-D velocity vector, $\mathbf{v} \in [-1, 1]^2$, the frequency of the VCO at location $\mathbf{c}_n$ is

$$\theta_n = 8 + 1.6 \, \|\mathbf{v}\|_2 - 1.272 \, \mathbf{c}_n \cdot \mathbf{v} \tag{2}$$

where the distance from the origin, $\|\mathbf{c}_n\|$, ranges from -1 at one end of a propeller to 1 at the other end. This is similar in nature to that used in [2].

3.2 Phase Coupling

The stochastic nature of spiking neurons causes imperfect behaviour of the oscillators. If set to the same frequency and started in phase, perfect oscillators will remain in phase. However, slight errors in frequencies will cause them to drift out of phase as time progresses. This random dephasing can disrupt the phases of the oscillators to the point where the phase ramp is overwhelmed by noise.

We designed a phase-coupling method that maintains a linear progression in phase across each propellor, so that the increment in phase from one VCO to the next is the same everywhere. The coupling method is described more completely in [17]. Briefly, each pair of adjacent VCOs is joined by a coupling node, called a *phase-step* node, which computes the phase difference between its two VCOs. All the phase-step nodes are interconnected and arrive at a consensus phase difference (the weighted average). After computing the phase error for each VCO, each phase-step node sends back a correction to keep the VCOs in the correct phase relationship.

While the phase-step nodes keep the phase linear within a 1-D propellor, we still need a way to ensure that all the phase ramps are coplanar. For example, drift could cause one propellor to attain a disproportionately steep slope that makes it tilt out of the plane delineated by the other propellors.

A more complex form of coupling is required to keep the phases coplanar with each other. We need to couple together three phase-step nodes (from three different propellors). The resulting phase adjustments are fed back to the phase-step nodes. Finally, we also used a phase-coupling node to keep the DC nodes of the three propellors in sync.

3.3 Simulation of Rat Motion

We created our network model to test some specific aspects of the Fourier model. In particular, we wanted to see if we would find grid cells that fired spikes on a hexagonal grid of locations. We also wanted to see if these grid cells would exhibit phase precession compared to a global theta cycle. We added a 2-D

VCO node that oscillates at approximately 8 Hz, and used this node's state as the authoritative theta cycle.

To simulate the movement of a rat in a circular environment, we added to our model a random-walk function that adjusts the velocity vector smoothly. The resulting simulated rat trajectories are shown later. One could predict the rat's location by numerically integrating the rat's velocity. However, the rat's own perceived location (as encoded in the phase ramp of the EC VCOs) soon drifted away from the computed position. A real rat seems to avoid this problem by updating its perceived location with sensory information [5]. Though we did not incorporate sensory input in our model here, our companion paper [17] presents an extension that does.

3.4 Network Architecture

As shown in Fig. 5, the network consists of three "wheels" of nodes, along with a velocity node, DC phase-coupling node, a theta-cycle node, and an array of grid-cell nodes. Each wheel has three propellors at angles 0°, 120°, and 240° (though a full model would include more propellors per wheel). The first wheel contains 17 VCO populations per propellor. Each population has 300 LIF neurons and encodes a 3-D vector.

The phase-step wheel also has 3 propellors, but with 16 nodes per propellor (since they model the phase differences between the VCO nodes). Each phase-step population has 500 LIF neurons and encodes a 6-D vector as described in [17]. The coplanar coupling wheel mirrors the phase-step wheel, with each coplanar coupling node having 500 LIF neurons and encoding a 6-D vector.

The grid-cell array has 17 nodes, mirroring the 17 nodes in each of the VCO propellors. Each grid node contains 200 LIF neurons and encodes a 2-D vector of the sum of the phase vectors from the three corresponding VCOs. That is, each grid node receives the phase vectors from a triad of VCOs and simply adds them together.

The DC phase-coupler node has 500 LIF neurons and encodes a 6-D vector that duplicates the phases of the three DC nodes. The velocity node has 100 LIF neurons and encodes a 2-D vector. Finally, the theta-cycle node contains 500 LIF neurons and encodes a 2-D vector that oscillates at approximately 8 Hz. The recurrent connections of the theta-cycle population use a synaptic time constant of $\tau_s = 5\,\text{ms}$.

Unless otherwise specified, we used the following parameter values for all neurons: synaptic time constant $\tau_s = 5\,\text{ms}$, refractory period $\tau_{\text{ref}} = 2\,\text{ms}$, membrane time constant $\tau_{\text{m}} = 20\,\text{ms}$, spiking threshold $J_{\text{th}} = 1$, encoding vectors selected randomly (uniformly) from the unit hyper-sphere, neural gain and bias chosen to randomly (uniformly) sample the unit hyper-sphere of the representational space, with a maximum firing rate in the range 200-400 Hz.

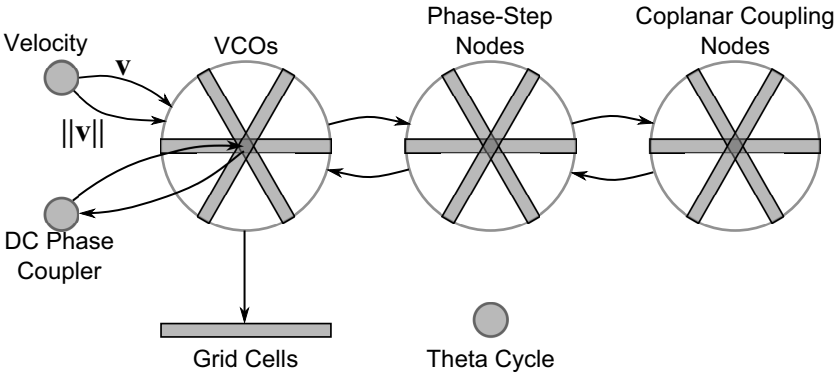

Fig. 5. Network overview. The velocity node modulates the frequency of the VCOs (see equation (2)). The phase-step nodes couple the VCOs to maintain a 1-D phase ramp within each propellor. The coplanar coupling nodes further keep the phase slopes of the different propellors linearly consistent (so that they all rest in a common plane). The DC phase coupler node keeps the absolute phase of the propellors in sync. The grid cells sum triads of VCOs. The theta cycle node is a stand-alone oscillator that maintains a frequency of approximately 8Hz.

4 Results

The simulations were run using the Nengo software package (nengo.ca). The whole model includes 119 nodes, for a total of 68,700 LIF neurons. We ran the model for 300 seconds simulation time. The execution of the model took about 110 minutes to run on a laptop with a 2.9GHz Intel Core i7 processor and 8GB of RAM.

4.1 Grid Cells

Figure 6 shows a sampling of grid cells, with their spikes superimposed overtop of the rat's trajectory. In the figure, the frequency of the grid-cell triad increases from left to right. The red dots of spikes clearly occur on a hexagonal grid with different scales. Not all neurons in the grid nodes exhibited grid firing patterns. However, about 10% did.

4.2 Theta-Phase Precession

If we focus on the timing of the grid-cell spike bursts, we can see that the start of the bursts precess through the theta cycle. Figure 7 plots the spikes as red lines over the theta cycle produced by the "theta" node. The frequency of oscillation for the VCOs – and hence the grid cells – is higher than the nominal 8Hz theta cycle. Thus, we see the bursts of grid-cell activity precess through the lower-frequency theta cycle.

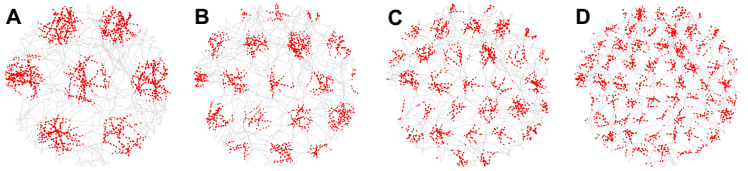

Fig. 6. Spikes from grid cells superimposed on the rat's trajectory. All the grid cells were taken from triads with an orientation of 0°. The neuron in A is from a grid-cell node at position 2 (where the central, or DC, grid-cell node is index 0). The neurons in B, C and D are from grid-cell nodes 3, 4 and 6, respectively.

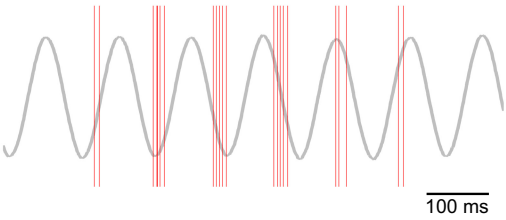

Fig. 7. Theta-phase precession of grid-cell spikes

5 Discussion

The model proposed in this paper was inspired by [2], but we re-formulated that approach into a coherent framework that allows for further analysis and deeper understanding. Part of our contribution is to envision the bank of VCOs organized in a polar fashion throughout the frequency domain. Movement of the animal induces frequency changes of those VCOs according to where they rest in the frequency domain. In this polar format, the VCO phases form a ramp. The slope of this ramp encodes the rat's location, and can be used as such when applied to a set of Fourier coefficients.

The connections from the VCOs to the spatial-map nodes represent Fourier coefficients. Thus, projecting the VCO phases through these connections results in a spatial map with the correct positional context. All the spatial maps are shifted in concert with the animal's motion.

Grid cells might emerge as a by-product of a phase coupling mechanism. Some research has shown that the distributed nature of grid-cell encoding offers better accuracy than the same number of sparse place cells [18]. But this theory still does not address why grid cells appear, since the bank of VCOs also offers a distributed representation of location. Another theory, and one that we plan to investigate, is that grid cells are a by-product of the coupling mechanisms that maintain the phase relationships within the bank of VCOs. It seems intuitive that place cells could offer a stable and accurate representation of location as long as the underlying network that feeds into the place cells encodes location in a stable and accurate manner. Coupling between nodes harnesses the redundancy in the

network and enables resources to be focussed on lower-dimensional data, such as location. The coplanar-coupling nodes assess the linear consistency among three or more other nodes. In general, a linearity constraint in 2-D will always require input from at least three VCOs (in addition to the implicitly included DC node). We plan to investigate more general implementations of the coplanar constraint and observe whether these mechanisms inherently generate grid-cell behaviours.

The network we have built involves 119 populations, and contains a total of 67,800 LIF neurons. Our implementation is an important step in demonstrating the capabilities and behaviours of our model. However, an obvious question remains, how might such a system get established? What self-organizing principles might apply, and where? Spatial maps of place cells have been learned using Hebbian learning [19]. Grid cells can emerge spontaneously in a topographically connected network with local excitation and lateral inhibition [7,10]. However, these "Turing grids" are not found in adults, leading researchers to suggest that they form during a developmental stage and are used to guide the formation of grid cells in the non-topographical, adult EC network. Even a random selection of grid cells can produce place cells [8,20]. We plan to investigate unsupervised and supervised learning algorithms to derive neural oscillators. One could also look at how such oscillators could take on the proper phase coupling.

6 Conclusion

Although a number of theories have been forwarded regarding the relationships between place cells, grid cells, phase precession, and other spatial-map cells, none have explained all the components with a single overarching framework. Our Fourier model of the entorhinal cortex path integration system organizes the pieces into an architecture with a rich and well-understood foundation. Knowledge about other properties of the Fourier Transform can help to guide further development of the model, and assess how it may (or may not) be extended to explain or predict other observations.

Acknowledgement. We are grateful for the support of the Natural Sciences and Engineering Research Council of Canada (NSERC), the Canada Foundation for Innovation (CFI), and the Ontario Innovation Trust.

References

1. Hafting, T., Fyhn, M., Molden, S., Moser, M., Moser, E.: Microstructure of a spatial map in the entorhinal cortex. Nature 436(7052), 801–806 (2005)
2. Welday, A.C., Shlifer, I.G., Bloom, M.L., Zhang, K., Blair, H.T.: Cosine Directional Tuning of Theta Cell Burst Frequencies: Evidence for Spatial Coding by Oscillatory Interference. Journal of Neuroscience 31(45), 16157–16176 (2011)
3. Moser, E., Kropff, E., Moser, M.: Place cells, grid cells, and the brain's spatial representation system. Annu. Rev. Neurosci. 31, 69–89 (2008)
4. Blair, H., Gupta, K., Zhang, K.: Conversion of a phase- to a rate-coded position signal by a three-stage model of theta cells, grid cells, and place cells. Hippocampus 18(12), 1239–1255 (2008)

5. Burgess, N., Barry, C., O'Keefe, J.: An oscillatory interference model of grid cell firing. Hippocampus 17(9), 801–812 (2007)
6. Krupic, J., Burgess, N., O'Keefe, J.: Neural Representations of Location Composed of Spatially Periodic Bands. Science 337(6096), 853–857 (2012)
7. Fuhs, M.C., Touretzky, D.S.: A spin glass model of path integration in rat medial entorhinal cortex. The Journal of Neuroscience 26(16), 4266–4276 (2006)
8. Solstad, T., Moser, E., Einevoll, G.T.: From grid cells to place cells: a mathematical model. Hippocampus 16(12), 1026–1031 (2006)
9. O'Keefe, J., Burgess, N.: Dual phase and rate coding in hippocampal place cells: theoretical significance and relationship to entorhinal grid cells. Hippocampus 15(7), 853–866 (2005)
10. McNaughton, B., Battaglia, F.P., Jensen, O., Moser, E., Moser, M.: Path integration and the neural basis of the 'cognitive map'. Nature Reviews Neuroscience 7(8), 663–678 (2006)
11. Blair, H., Welday, A.C., Zhang, K.: Scale-Invariant Memory Representations Emerge from Moire Interference between Grid Fields That Produce Theta Oscillations: A Computational Model. Journal of Neuroscience 27(12), 3211–3229 (2007)
12. Zilli, E.A.: Models of grid cell spatial firing published 2005–2011. Frontiers in Neural Circuits 6(16), 1–17 (2012)
13. Conklin, J., Eliasmith, C.: A Controlled Attractor Network Model of Path Integration in the Rat. Journal of Computational Neuroscience 18, 183–203 (2005)
14. Koch, C.: Simplified models of individual neurons. Biophysics of computation (1999)
15. Eliasmith, C., Anderson, C.H.: Neural engineering: Computation, representation, and dynamics in neurobiological systems. MIT Press, Cambridge (2003)
16. Eliasmith, C., Stewart, T.C., Choo, X., Bekolay, T., DeWolf, T., Tang, C., Rasmussen, D.: A Large-Scale Model of the Functioning Brain. Science 338(6111), 1202–1205 (2012)
17. Ji, X., Kushagra, S., Orchard, J.: Sensory updates to combat path-integration drift. In: Zaïane, O., Zilles, S. (eds.) Canadian AI 2013. LNCS (LNAI), vol. 7884, pp. 263–270. Springer, Heidelberg (2013)
18. Mathis, A., Herz, A.: Optimal Population Codes for Space: Grid Cells Outperform Place Cells. Neural Computation 24, 2280–2317 (2012)
19. Rolls, E.T., Stringer, S.M., Elliot, T.: Entorhinal cortex grid cells can map to hippocampal place cells by competitive learning. Network: Computation in Neural Systems 17(4), 447–465 (2006)
20. de Almeida, L., Idiart, M., Lisman, J.E.: The input–output transformation of the hippocampal granule cells: from grid cells to place fields. The Journal of Neuroscience 29(23), 7504–7512 (2009)